Fire Safety Journal 46 (2011) 568–578

Contents lists available at SciVerse ScienceDirect

Fire Safety Journal

journal homepage: www.elsevier.com/locate/firesaf

Experimental investigation of structure vulnerabilities to firebrand showers

Samuel L. Manzello [a,*], Seul-Hyun Park [a,1], Sayaka Suzuki [a], John R. Shields [a], Yoshihiko Hayashi [b]

[a] Fire Research Division, Engineering Laboratory, National Institute of Standards and Technology, 100 Bureau Drive, Gaithersburg, MD 20899-8662, USA
[b] Department of Fire Engineering, Building Research Institute (BRI), 1 Tachihara, Tsukuba, Ibaraki 305-0802, Japan

ARTICLE INFO

Article history:
Received 24 August 2011
Accepted 10 September 2011
Available online 29 September 2011

Keywords:
Firebrands
Ignition
WUI fires

ABSTRACT

Attempting to experimentally quantify the vulnerabilities of structures to ignition from firebrand showers has remained elusive. The coupling of two facilities has begun to unravel this difficult problem. The NIST Firebrand Generator (NIST Dragon) is an experimental device that can generate a firebrand shower in a safe and repeatable fashion. Since wind plays a critical role in the spread of WUI fires in the USA and urban fires in Japan, NIST has established collaboration with the Building Research Institute (BRI) in Japan. BRI maintains one of the only full scale wind tunnel facilities in the world designed specifically for fire experimentation; the Fire Research Wind Tunnel Facility (FRWTF). The present investigation is aimed at extensively quantifying firebrand penetration through building vents using full scale tests. A structure was placed inside the FRWTF and firebrand showers were directed at the structure using the NIST Dragon. The structure was fitted with a generic building vent, consisting of only a frame fitted with a metal mesh. Six different mesh sizes openings were used for testing. Behind the mesh, four different materials were placed to ascertain whether the firebrands that were able to penetrate the building mesh assembly could ignite these materials. Reduced scale test methods afford the capability to test new vent technologies and may serve as the basis for new standard testing methodologies. As a result, a new experimental facility developed at NIST is presented and is known as the NIST Dragon's LAIR (Lofting and Ignition Research). The NIST Dragon's LAIR has been developed to simulate a wind driven firebrand attack at reduced scale. The facility consists of a reduced scale Firebrand Generator (Baby Dragon) coupled to a bench scale wind tunnel. Finally, a series of full scale experiments were conducted to visualize the flow of firebrands around obstacles placed downstream of the NIST Dragon. Firebrands were observed to accumulate in front of these obstacles at a stagnation plane, as was observed when the structure was used for firebrand penetration through building vent experiments, due to flow recirculation. The accumulation of firebrands at a stagnation plane presents a severe threat to ignitable materials placed near structures.

Published by Elsevier Ltd.

1. Introduction

The rapid growth of the Wildland–Urban Interface (WUI) in the USA has put an increasing number of communities at risk to fires originating from wildland fuels [1]. As an example of this, the Southern California WUI fires in 2007 displaced nearly 300,000 people, destroyed over 1000 structures, and resulted in $1B paid by insurers in 2007 alone [1].

As vegetation and structures burn in WUI fires, pieces of burning material, known as firebrands, are generated, become lofted and get carried by the wind resulting in structures being bombarded by firebrands during these fires. Anecdotal evidence as well as post-fire damage assessment studies suggests that wind driven firebrand attack is responsible for the majority of structure ignitions in WUI fires [2–3]. One approach to mitigate firebrand ignition of structures is to design new homes and retrofit homes to be more resistant to firebrand ignition. To do this, building codes and standards are needed to guide construction of new structures in areas known to be prone to WUI fires in order to reduce structural ignition in the event of a firebrand attack. In order to develop such standards requires a thorough scientific methodology to understand the types of building materials that can be ignited by firebrands as well as vulnerable points on a structure where firebrands may easily enter.

Unfortunately, it is not a simple exercise to develop experimental methods to replicate firebrand bombardment of structures observed in actual WUI fires. Furthermore, past firebrand studies [4–17] have been focused on attempting to predict spotting distances, namely how far firebrands travel. Naturally, such investigations do not address the vulnerabilities of structures from ignition due to firebrand showers. Therefore, completely new experimental methods are required to understand structure vulnerability to wind driven firebrand showers.

* Corresponding author. Tel.: +1 301 975 6891; fax: +1 301 975 4052.
E-mail address: samuelm@nist.gov (S.L. Manzello).
[1] Space Application & Future Technology Center Korea Aerospace Research Institute (KARI), Deajeon 305-333, South Korea.

0379-7112/$ - see front matter Published by Elsevier Ltd.
doi:10.1016/j.firesaf.2011.09.003

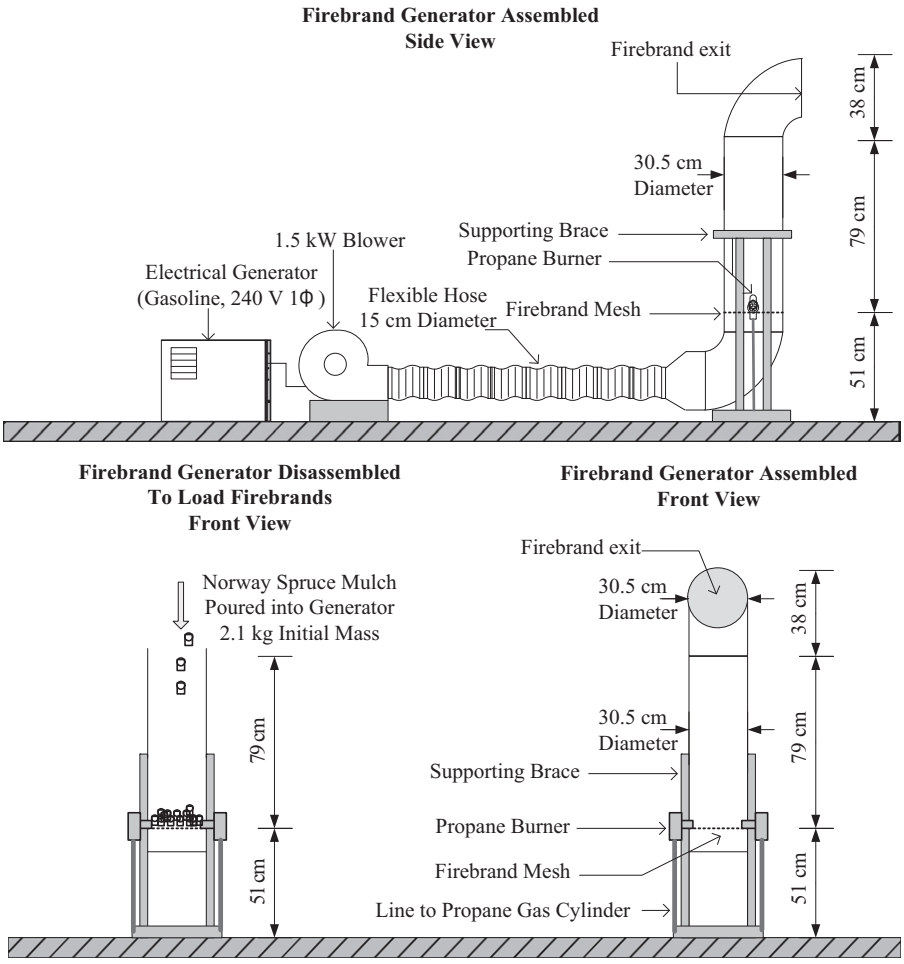

Fig. 1. Side and front view drawings of NIST Firebrand Generator (Dragon) used for full scale tests.

To this end, an experimental apparatus, known as the NIST Firebrand Generator (NIST Dragon), has been constructed to generate a controlled and repeatable size and mass distribution of glowing firebrands. Since wind plays a critical role in the spread of WUI fires in the USA and urban fires in Japan, NIST established collaboration with the Building Research Institute (BRI) in Japan in 2006. BRI maintains one of the only full scale wind tunnel facilities in the world designed specifically for fire experimentation; the Fire Research Wind Tunnel Facility (FRWTF). Although a dearth of information exists regarding actual firebrand exposures in real WUI fires, the full scale experiments conducted recently by NIST at BRI's FRWTF attempt to simulate wind driven firebrand bombardment. In simulating firebrand showers to 10 m/s, these large scale experiments have provided insight into structure vulnerabilities under firebrand attack [18–20].

The present investigation is aimed at extensively quantifying firebrand penetration through building vents using full scale tests at BRI. These new full scale experiments greatly expand upon prior BRI/NIST work that considered firebrand penetration into building vents [18]. In prior work, firebrand penetration into a gable vent fitted with a mesh assembly (only three mesh sizes were used—6.0, 3.0, and 1.5 mm) was investigated and shredded paper was placed behind the mesh to determine if firebrands that penetrated the vent and subsequent mesh were able to produce an ignition event [18]. In this study, six different mesh sizes were considered, from 5.72 to 1.04 mm opening, as well as four different types of ignitable materials placed inside the structure. This greater range of parameters allowed for the generation of a database of firebrand penetration behavior and subsequent ignition of materials placed behind varying mesh sizes.

While full scale tests are necessary to highlight vulnerabilities of structures to firebrand showers, reduced scale test methods afford the capability to test new vent technologies and may serve as a basis for new standard testing methodologies. As a result, a new experimental facility was developed, known as the NIST Dragon's LAIR (Lofting and Ignition Research). The NIST Dragon's LAIR has been developed to simulate a wind driven firebrand attack at reduced scale. The facility consists of a reduced scale Firebrand Generator (Baby Dragon) coupled to a bench scale wind tunnel. A comparison testing protocol was undertaken to determine if the reduced scale method was capable of capturing firebrand penetration through building vents and subsequent ignition of materials placed behind the vent that was observed using the full scale test experiments conducted at BRI in Japan. These experiments have been described in a recently released NIST report and conference publication [21–22]. This paper greatly expands on the analysis presented there.

Finally, another series of full scale experiments, presented for the first time, were conducted to visualize the flow of firebrands around obstacles placed downstream of the NIST Dragon. While structures possess vulnerabilities to firebrand showers (*e.g.* building vents and roofing assemblies), it was desired to determine if firebrands have the potential to accumulate in front of structures and ignite materials placed near structures.

2. Experimental description

2.1. Full scale experiments

2.1.1. Building vent vulnerabilities

Fig. 1 is a drawing of the NIST Firebrand Generator. A brief description of the device is provided here for completeness and follows prior descriptions very closely [18–20]. This version of the Firebrand Generator derives from the first-generation, proof-of-concept device [23]. The bottom panel displays the procedure for loading the Norway Spruce (*picea abies Karst)* tree mulch into the apparatus. Norway Spruce mulch was used in prior work using the Firebrand Generator and the justification for this type of mulch is provided elsewhere [20–21].

The mulch pieces were deposited into the Firebrand Generator by removing the top portion. The mulch pieces were supported using a stainless steel mesh screen (0.35 cm spacing). Two different screens were used to filter the mulch pieces prior to loading into the Firebrand Generator. The first screen blocked all mulch pieces larger than 25 mm in diameter. A second screen was then used to remove all needles from the mulch pieces. The justification for this filtering methodology is provided below. The mulch loading was fixed at 2.1 kg. The Firebrand Generator was driven by a 1.5 kW blower.

After the Norway Spruce tree mulch was loaded, the top section of the Firebrand Generator was coupled to the main body of the apparatus. The blower was then started to provide a low flow for ignition (1.0 m/s flow inside the duct measured upstream of the wood pieces). The two propane burners were then ignited individually and simultaneously inserted into the side of the device. The Norway Spruce mulch was exposed to the igniter for a total of 45 s. After 45 s, the fan speed of the blower was increased (2.0 m/s flow inside the duct measured upstream of the wood pieces). This sequence of events was selected to generate a continuous flow of glowing firebrands for approximately four minutes duration.

The Firebrand Generator was installed inside the test section of the FRWTF at BRI. Fig. 2 displays a layout of the facility. The facility used a 4.0 m diameter fan to produce the wind field and was capable of producing a flow of 10 m/s. The wind flow velocity distribution was measured using a 21 point hot wire anemometer array. To track the evolution of the size and mass distribution of firebrands produced, a series of rectangular pans (water-filled) were placed downstream of the Firebrand Generator. Each pan was 49.5 cm long by 29.5 cm wide. The arrangement and width of the pans was not random; rather it was based on scoping experiments to determine the locations where the firebrands would most likely land. After the experiments were completed, the firebrands were filtered from the water using a series of fine mesh filters. The firebrands were subsequently dried in an oven at 104 °C for eight hours. The firebrand sizes were then measured using precision calipers ($\frac{1}{100}$ mm resolution). Following size determination, the firebrands were then weighed using a precision balance (0.001 g resolution). For each experiment, more than 100 firebrands were collected, dried, and measured. These experiments (three replicate tests) were conducted separately from the ignition tests.

Fig. 3 is a detailed drawing of the front face of the target structure showing the location of the vent opening. The overall dimensions of the structure were 3.06 m in height, 3.04 m in width, and 3.05 m in depth. The structure was constructed of calcium silicate (non-combustible) board. A generic building vent design (consisting of only a frame fitted with a metal mesh) was used since the purpose of the experiments was to assess the proposed test methods and not specific proprietary vent technology. The vent opening was fitted with six different types of metal mesh: 4×4 mesh $\times$ 0.64 mm wire diameter, 8×8 mesh $\times$ 0.43 mm wire diameter, 10×10 mesh $\times$ 0.51 mm wire diameter, 14×14 mesh $\times$ 0.23 mm wire diameter, 16×16 mesh $\times$ 0.23 mm wire diameter, and 20×20 mesh $\times$ 0.23 mm wire diameter. These mesh sizes corresponded to opening sizes of: 5.72 mm (4×4), 2.74 mm (8×8), 2.0 mm (10×10), 1.55 mm (14×14), 1.35 mm (16×16), and 1.04 mm (20×20). These opening sizes were obtained from the manufacturer and subsequently

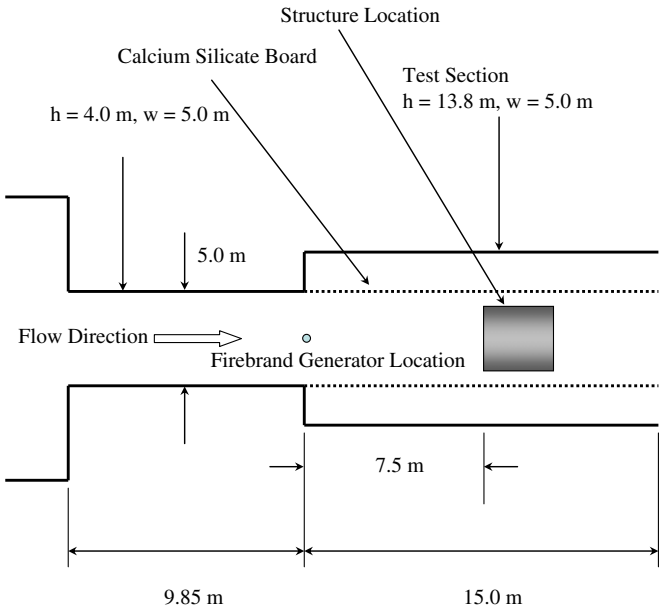

Fig. 2. Drawing of the FRWTF (top view). The location of the Firebrand Generator is shown as well as the structure used for testing. The structure was intentionally constructed of calcium silicate board (non-combustible).

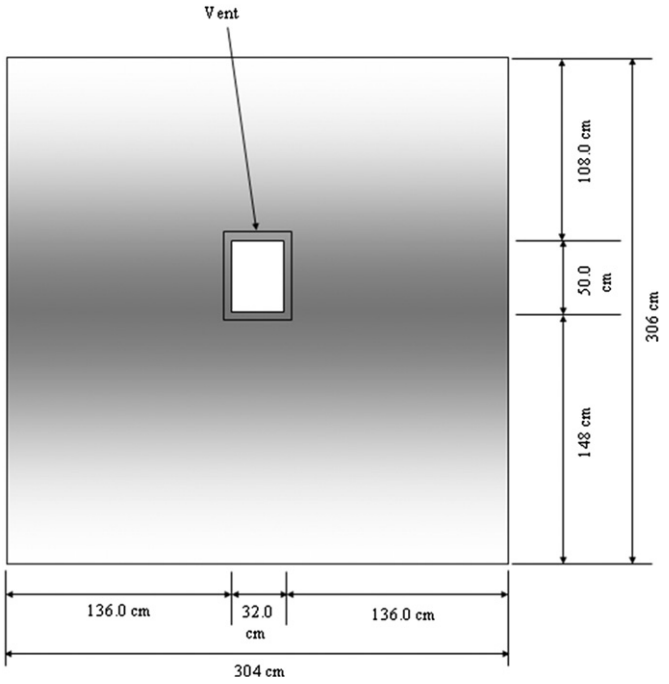

Fig. 3. Schematic of structure used. The vent opening is shown where the mesh was placed.

verified using measurements at NIST. Mesh was defined, per the manufacturer, as the number of openings per 25.4 mm (1″).

For building ventilation, common vents include gable vents, foundation vents, and eave or soffit vents. Gable vents and eave vents are used for attic ventilation and foundation vents are used to provide air flow to crawl space areas. Prior to conducting the experiments, computer simulations were conducted using the NIST Fire Dynamics Simulator (FDS) to visualize the flow around the structure in the FRWTF [24]. FDS is a computational fluid dynamics model of fire-driven fluid flow and numerically solves a form of the Navier–Stokes equations appropriate for low-speed, thermally driven flow. While FDS was designed with fire in mind, it may be used, as in the case of the simulations conducted in this study, for low-speed fluid flow simulations that do not involve fire [24].

Since eave vents, as the name suggests, are placed horizontally under an eave, simulations were performed to compare air flow profiles of a vent placed under an eave as compared to a vent placed vertically, such as a foundation or gable vent. Clearly, for a vent placed under an eave, the simulations demonstrated that a great deal of flow recirculation exists, implying less likelihood for firebrands to actually arrive at such a location. On the other hand, for a vent placed vertically and not under an eave, it is far easier for air flow to arrive less perturbed at this location. As a result, the placement of the mesh assembly, on the front face of the structure, was intentionally selected to provide an intense flux of firebrands from the NIST Firebrand Generator. It also allowed comparison to prior BRI/NIST work that considered a gable vent fitted with a mesh assembly [18].

Behind the mesh, four different materials were placed to ascertain whether the firebrands that were able to penetrate the building mesh assembly could ignite these materials. The materials were shredded paper, cotton, crevices constructed with oriented strand board (OSB), and wood (to form 90° angle). For the crevice tests, experiments were conducted with the crevice filled with or without shredded paper. The purpose of using the crevice was to determine if firebrands that penetrated the mesh were able to ignite building materials. Paper in the crevice was intended to simulate fine fuel debris. To simplify comparisons, all materials were oven dried in these experiments and care was taken to ensure consistency with the testing materials used for full scale tests and reduced scale tests. All of the materials used for ignition testing were placed 19 cm below the mesh assembly inside the structure.

Inside the structure, behind the mesh, a screen was placed to direct firebrands that penetrated the mesh towards the ignitable materials. Without a guide, the firebrands that penetrated the mesh would simply land in various places inside the structure. The purpose of these experiments was to create a worst case scenario; directing the firebrands that penetrated the mesh on to or toward the ignitable materials.

2.1.2. Firebrand accumulation in front of obstacles

In these experiments, the NIST Dragon was fed with mulch in an identical manner described above, but rather than the full structure, an obstacle was placed downstream of the firebrand showers inside the FRWTF. The same obstacle was oriented differently to have a different aspect ratio and thus allow for qualitative comparison of firebrand flow and the resulting stagnation plane where firebrands may potentially accumulate. When oriented lower to the ground, the obstacle dimensions were 1.0 m high and 2.0 m wide; for a higher orientation, the obstacle dimensions were 2.0 m high and 1.0 m wide. The front face of the obstacle was constructed from calcium silicate board. The distance of the NIST Dragon from the obstacles was the same as the structure experiments, namely 7.5 m downstream. In front of the obstacles, a series of wood boards (thickness of 9 mm) were placed flat on the ground of the FRWTF to determine if the accumulated firebrands were able to produce ignition events. The wood boards were not oven dried (moisture content 11% dry basis) in order to provide the accumulated firebrands a greater barrier to produce ignition in these materials. A total of six experiments were conducted; three replicate tests for each obstacle orientation.

2.2. Reduced scale experiments—NIST Dragon's LAIR facility

Fig. 4 is a schematic of the NIST Dragon's LAIR (Lofting and Ignition Research) facility. The Dragon's LAIR consisted of a reduced scale Firebrand Generator (Baby Dragon) coupled to a reduced scale wind tunnel (see Fig. 4).

To produce firebrands, the Baby Dragon was fed with wood pieces. For all reduced scale tests, Douglas-Fir wood pieces machined with dimensions of 7.9 mm (H) by 7.9 mm (W) by 12.7 mm (L) were used. The total initial mass was fixed at 150 g for all tests. The reason for using wood pieces for the reduced scale tests, as opposed to mulch is described in detail elsewhere [21].

After the wood pieces were loaded, the window of the wind tunnel was closed, the desired wind tunnel flow was set, and the blower was then started to provide a low flow for ignition. One propane burner was ignited and simultaneously inserted into the side of the generator. The burner was maintained for a total time

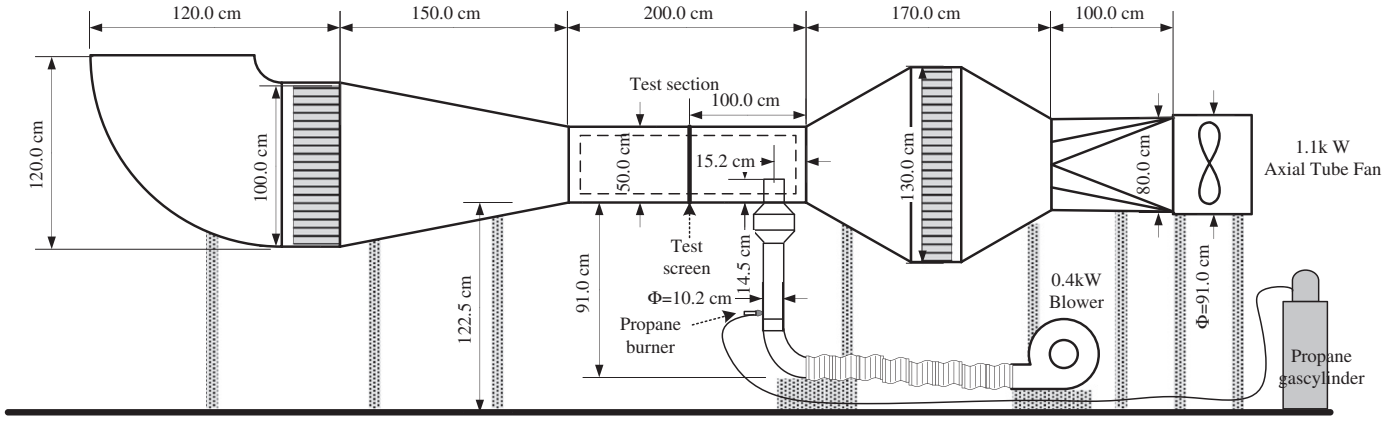

Fig. 4. Schematic of Dragon's LAIR Facility. The Baby Dragon (coupled to 0.4 kW blower) as well as the firebrand seeding locating into the wind tunnel are shown.

of 40 s. This sequence of events was selected in order to generate a continuous flow of glowing firebrands for approximately four minutes duration and resulted in little or no smoke production.

The test section of the wind tunnel was 50 cm × 50 cm × 200 cm. The flow was provided by an axial fan 91 cm in diameter. To track the evolution of the size and mass distribution of firebrands produced, a series of water pans was placed downstream of the Baby Dragon. After the experiments were completed, the pans were collected and the firebrands were filtered from the water using a series of fine mesh filters. The firebrands were subsequently dried in an oven at 104 °C for eight hours. The firebrand sizes were then measured using precision calipers ($\frac{1}{100}$ mm resolution). Following size determination, the firebrands were then weighed using a precision balance (0.001 g resolution). These experiments (three replicate tests) were conducted separately from the ignition tests.

The same mesh sizes described for the full scale tests (see section above) were used. Each mesh was mounted in a metal mounting bracket with the same effective area as the full scale tests (1600 cm^2). The mesh was placed 100 cm downstream of the test section. Behind the mesh, the same ignitable materials used in the full scale tests were placed; namely shredded paper, cotton, crevices constructed with oriented strand board (OSB), and wood (to form 90° angle; with and without shredded paper).

3. Results

3.1. Building vent vulnerabilities

The Firebrand Generator was designed to produce firebrands characteristic to those produced from burning trees [25–26]. In this study, the input conditions for the Firebrand Generator were intentionally selected to produce firebrands with masses as large as 0.2 g. This was accomplished by sorting the Norway Spruce tree mulch using a series of filters prior to being loaded into the Firebrand Generator (as described above). A similar filtering procedure was used previously when other conifer species were used as the mulch source [18–19]. The size and mass distribution of firebrands produced using the Firebrand Generator is displayed in Fig. 5a. The total mass of firebrands produced was also determined based on repeat experiments. With mulch loadings of 2.1 kg, an average of 196 g (varied from 192 to 200 g) of glowing firebrands were produced. Therefore, the total mass of firebrands directed at the structure for each experiment was quite repeatable.

For the full scale tests, the wind tunnel speed was fixed at 7 m/s (±10%). For each mesh tested, the velocity was measured behind the mesh (at the centerline) using a hot wire anemometer. The velocity behind the mesh varied from 7 m/s (4 × 4 mesh; 5.72 mm opening) to 5 m/s (20 × 20 mesh; 1.04 mm opening). The uncertainty in these measurements is ±10%. Fig. 6 displays a picture of a typical experiment. In this particular experiment, the mesh used was 20 × 20 (1.04 mm).

An important factor to consider for the full scale tests was that while the Firebrand Generator produced a large number of firebrands, all of these firebrands do not actually arrive at the mesh location due to flow recirculation produced by the presence of the structure. To quantify the distribution of firebrands arriving at the mesh area as a function of time, experiments were conducted using the 20 × 20 (1.04 mm) mesh, since this mesh size initially trapped all firebrands on it prior to their continuous burning and ultimate penetration through the mesh. This allowed for the ability to simply count the time varying number of firebrands arriving at the given mesh area.

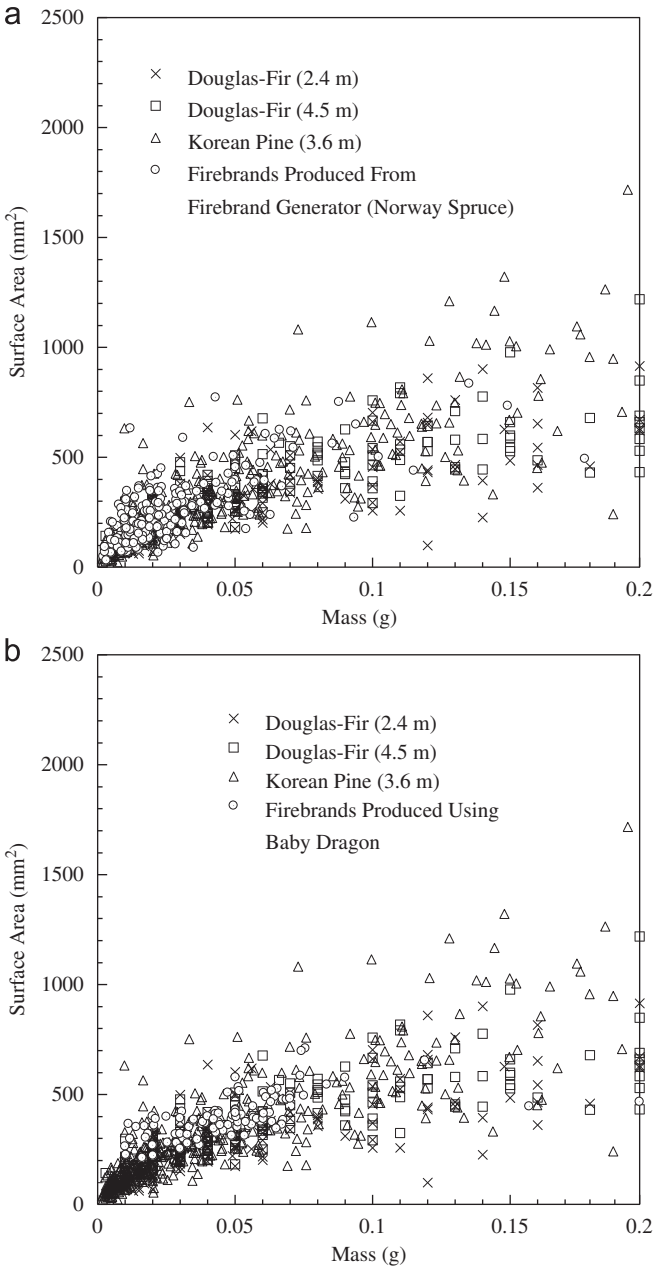

Fig. 5. (a) Firebrands produced from burning trees compared to those produced using the Firebrand Generator. The uncertainty in determining the surface area is ±10% and (b) firebrands produced from burning trees compared to those produced using the Baby Dragon.

To accomplish this in an efficient manner, image analysis was performed. To distinguish glowing firebrands from the uneven background required correcting the uneven illumination across the images by offsetting the background and then a 3 × 3 average spatial filter was applied to reduce the image noise. A typical image of glowing firebrands deposited on the 20 × 20 mesh and a processed image generated by background offsetting and filtering are displayed in Fig. 7a and b, respectively. To further aid image processing, the image shown in Fig. 7b was converted into an 8-bit image. A binary image (that only consists of black and white pixels) was then produced from the 8-bit image by setting a fixed threshold value for the identification of glowing firebrands. All white pixels belonging to a same body was finally grouped as one firebrand in order to count the firebrand. In Fig. 7c, each of

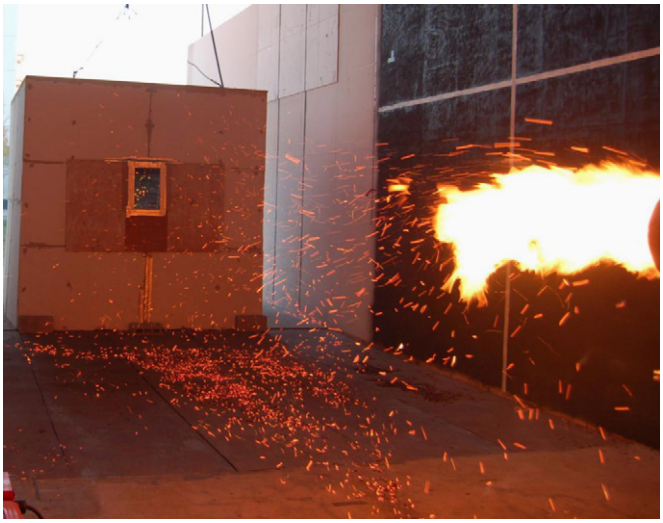

Fig. 6. Typical experiment using NIST Firebrand Generator at BRI's FRWTF. The mesh installed in this experiment was 20×20 (1.04 mm), the wind tunnel speed was 7 m/s, and the Firebrand Generator was located 7.5 m from the structure.

firebrands identified was counted and labeled. The data obtained from this analysis shown in Fig. 8.

Three repeat experiments were conducted for each of the four ignitable materials considered and the results are tabulated in Table 1. The acronyms in the table are as follows: NI—no ignition; SI—smoldering ignition; and FI—flaming ignition.

When shredded paper was used, a repeatable SI was observed for all mesh sizes up to 16×16 (1.35 mm). As the mesh size was reduced, the number of locations in the fuel bed where ignition was observed was reduced greatly. For example, for the 16×16 (1.35 mm) mesh, SI was observed only in one location in each of the repeat experiments. As for the smallest mesh size tested (20×20) (1.04 mm), SI was observed in only one experiment out of three. Subsequent repeats resulted in NI for this mesh size but the paper showed evidence of burns from firebrands. For several of the larger mesh sizes, the SI transitioned to FI. The shredded paper results are in agreement with prior BRI/NIST work using gable vents fitted with 6.0, 3.0, and 1.5 mm mesh [18].

For cotton, the ignition behavior was similar for all mesh sizes. The firebrands would deposit into the cotton bed and simply burn holes into the cotton. In several cases, the firebrands burned holes directly through the cotton samples. While a reduction in mesh size resulted in fewer holes in the cotton, ignition was never fully suppressed. A transition to FI was never observed. The shredded paper and cotton tests demonstrate that mesh size reduction was not effective in reducing ignition from firebrand showers for these full scale experiments.

The bare wood crevice experiments resulted in SI in the OSB layer for the 4×4 (5.72 mm) and 8×8 (2.74 mm) mesh sizes. As the mesh size was reduced to 10×10 (2.0 mm), the firebrands were not able to ignite the bare wood crevices.

When the crevices were filled with shredded paper, SI followed by FI occurred in the paper for mesh sizes up to 10×10 (2.0 mm). The OSB layer was then observed to ignite by SI and subsequently produced a self-sustaining SI that continued to burn holes into the OSB. For the smallest mesh sizes tested (16×16 and 20×20), NI was observed in the paper and consequently NI in the crevice. The results of an experiment conducted using 10×10 (2.0 mm) mesh are shown in Fig. 9.

Experiments were also conducted where the temperature was measured at the location of the fuel bed to investigate whether there was any pre-heating during the experiments. The source of any potential pre-heat was the heat generated by the Firebrand Generator. The temperature rise measured at the fuel bed was on the order of 3 °C.

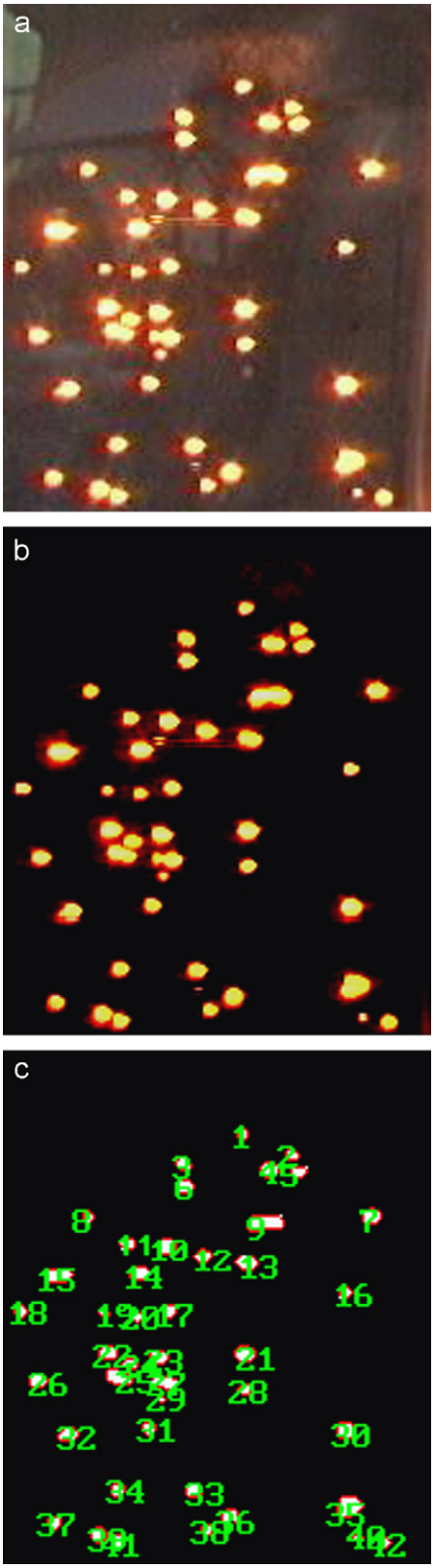

Fig. 7. (a) Raw image of firebrands deposited on 20×20 (1.04 mm); (b) processed image generated by background offsetting and filtering, and (c) images showing firebrands counted using processed image.

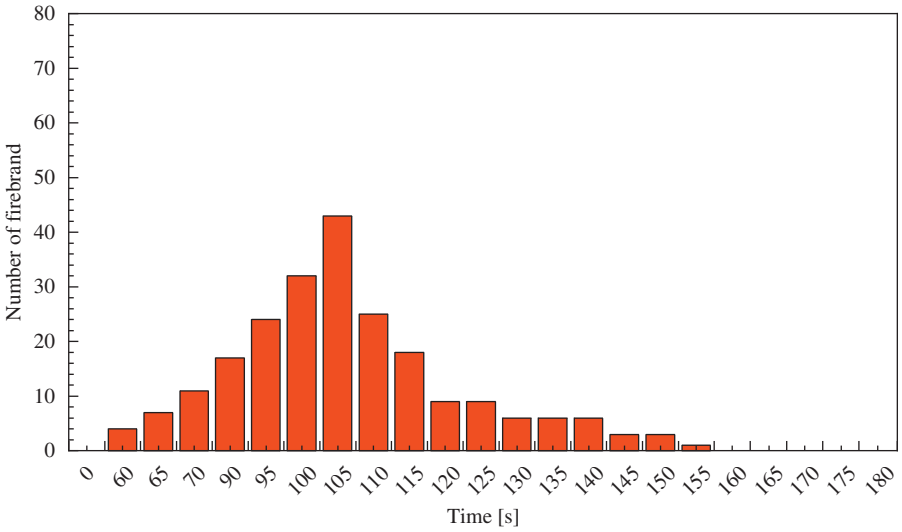

Fig. 8. Number of firebrands arriving on the mesh as a function of time for the full scale experiments. The mesh area was 1600 cm^2. At each time, the number of firebrands plotted in the figure was based on the average of three repeat experiments. The relative variation in the average number of firebrands measured was similar for all times (less than 20%).

Table 1
Summary of full scale tests at BRI. A total of 72 experiments were conducted.

Mesh	Paper	Cotton	Crevice	Crevice with paper
4×4 (5.72 mm)	SI–FI	SI	SI	SI–FI (paper)SI (OSB)
8×8 (2.74 mm)	SI–FI	SI	SI	SI–FI (paper) SI (OSB)
10×10 (2.0 mm)	SI–FI	SI	NI	SI–FI (paper) (SI OSB)
14×14 (1.55 mm)	SI	SI	NI	SI (paper) SI (OSB)
16×16 (1.35 mm)	SI	SI	NI	NI
20×20 (1.04 mm)	Two tests: NI; One test SI	Two tests: SI; One Test: NI	NI	NI

NI–no ignition; SI–smoldering ignition; and FI–flaming ignition.

Fig. 9. Images obtained (top view) for crevice filled with paper tests using 10×10 (2.0 mm) mesh.

3.2. Firebrand penetration through building vents—NIST Dragon's LAIR

Similar to the full scale experiments, the size and mass distribution of firebrands produced using the Baby Dragon was determined (see Fig. 5b). These sizes/masses were similar to firebrands produced using the NIST Firebrand Generator (see Fig. 5a). The total mass of firebrands produced using the Baby Dragon was also determined based on repeat experiments. With an initial loading of 150 g, an average of 12.2 g (varied from 11 to 13.6 g) of glowing firebrands were produced. Therefore, the total mass of firebrands directed at the mesh was repeatable for each experiment.

In the reduced scale tests, all firebrands generated landed on the mesh. To quantify the distribution of firebrands arriving at the mesh area as a function of time, experiments were conducted using the 20×20 (1.04 mm) mesh since this mesh size initially trapped all firebrands on it prior to their eventual burn down and penetration through the mesh. This allowed for the ability to simply count the time varying number of firebrands arriving at the target mesh (same technique described above). This data is shown in Fig. 10.

To provide a meaningful comparison for the ignition studies, the velocity was matched behind the mesh for the reduced scale experiments to those velocities measured behind the mesh for the full scale tests. Fig. 11 displays a picture of a typical experiment using the Dragon's LAIR. In this particular image, the mesh used was 14×14 (1.55 mm). Three repeat experiments were conducted for each of the four ignitable materials and the results are tabulated in Table 2.

When shredded paper was used, a repeatable SI was observed for all mesh sizes up to 16×16 (1.35 mm). As the mesh size was reduced, the number of locations where ignition was observed in the shredded paper beds was reduced greatly. For example, for the 16×16 (1.35 mm) mesh, SI was observed only in one location in each of the repeat experiments. These results were identical to the full scale tests. As for the smallest mesh size tested (20×20; 1.04 mm), NI was observed in all experiments. The paper showed evidence of burns from firebrands but these did not produce self-sustaining SI. In the full scale tests, the shredded paper was observed to produce a SI in only one of the experiments for the

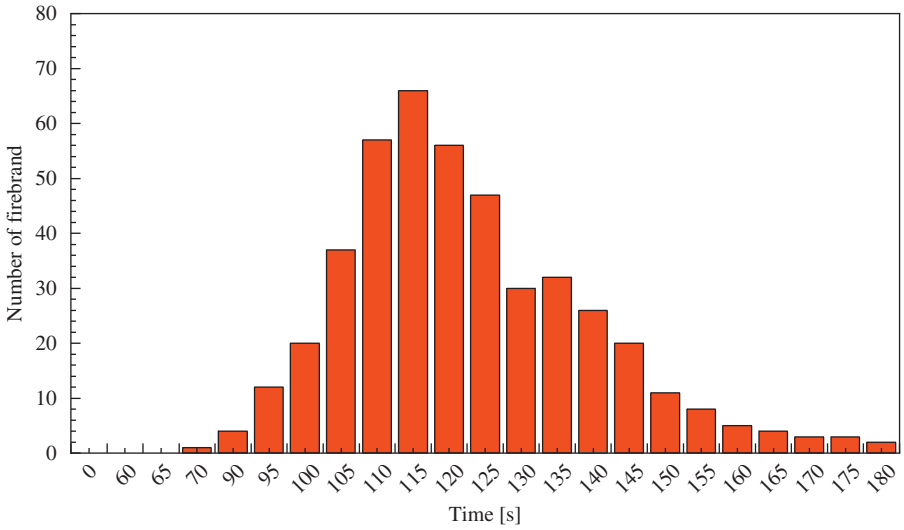

Fig. 10. Number of firebrands arriving on the mesh as a function of time for the reduced scale experiments. The mesh area is 1600 cm^2. The number of firebrands plotted in the figure, at each time, was based on the average of three repeat experiments. The relative variation in the average number of firebrands measured was similar for all times (less than 10%).

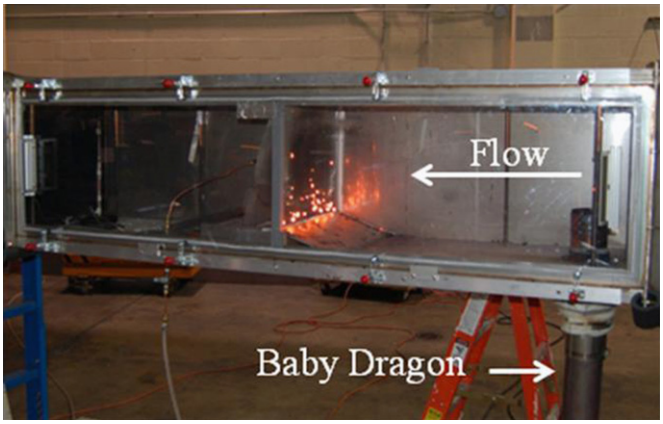

Fig. 11. Picture of typical experiment using the Dragon's LAIR. A 14×14 (1.55 mm) mesh was being used when this photograph was taken.

Table 2
Summary of reduced scale tests at NIST. A total of 72 experiments were conducted.

Mesh	Paper	Cotton	Crevice	Crevice with paper
4×4 (5.72 mm)	SI–FI	SI–FI	SI	SI–FI (paper) SI (OSB)
8×8 (2.74 mm)	SI–FI	SI	SI	SI–FI (paper) SI (OSB)
10×10 (2.0 mm)	SI–FI	SI	NI	SI–FI (paper) (SI OSB)
14×14 (1.55 mm)	SI	SI	NI	SI (paper) SI (OSB)
16×16 (1.35 mm)	SI	SI	NI	NI
20×20 (1.04 mm)	NI	SI	NI	NI

NI—no ignition; SI—smoldering ignition; and FI—flaming ignition.

Fig. 12. Image of firebrands flowing around one of the obstacles used.

20×20 (1.04 mm) mesh. For several of the larger mesh sizes, the SI transitioned to FI.

For cotton, the behavior was similar for all mesh sizes. The firebrands were deposited in the cotton bed and burned holes into the cotton. In several cases, the firebrand burned holes completely through the cotton samples. While a reduction in mesh size resulted in fewer holes in the cotton, ignition was never fully suppressed. The only notable difference between the reduced scale tests and full scale tests for cotton was a transition from SI to FI was observed for the largest mesh size tested (4×4; 5.72 mm). In the full scale tests, a transition from SI to FI was not observed for the largest mesh size.

The bare wood crevice experiments resulted in SI in the OSB layer for the 4×4 (5.72 mm) and 8×8 (2.74 mm) mesh sizes. As the mesh size was reduced to 10×10 (2.0 mm), the firebrands were not able to provide any ignition of the bare wood crevices. This behavior was the same as that observed in the full scale tests.

When the crevices were filled with shredded paper, SI followed by FI occurred in the paper for mesh sizes up to 10×10 (2.0 mm). The OSB layer was then observed to ignite by

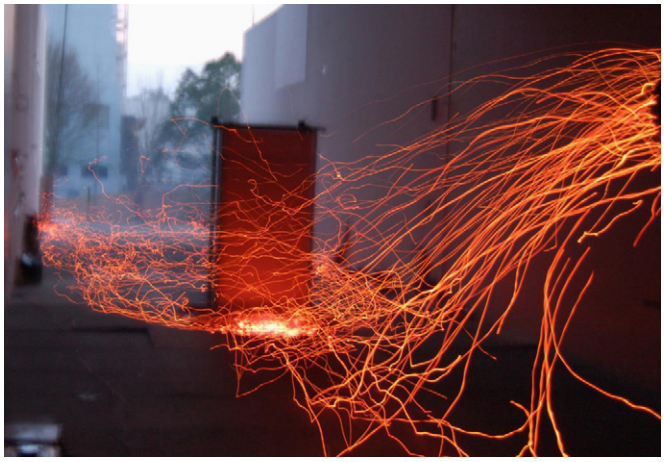

Fig. 13. Photograph taken by increasing the exposure time on the camera to visualize the firebrand flow process over the obstacles.

SI and subsequently produced a self-sustaining SI that continued to burn holes into the OSB. For the smallest mesh sizes tested (16×16 and 20×20), NI was observed in the paper and consequently NI in the crevice. These results were also the same as the full scale tests (described above).

Finally, experiments were also conducted in which the temperature was measured at the location of the fuel bed to investigate whether there was any pre-heating (by the Firebrand Generator) of the fuel bed during the experiments. The temperature rise measured at the full bed was on the order of 9 °C.

3.3. Firebrand accumulation in front of obstacles

Fig. 12 displays images of firebrands flowing around one of the obstacles used. As can be seen, the presence of the obstacle resulted in a stagnation plane where numerous firebrands were able to accumulate. After the firebrands were observed to accumulate, intense glowing combustion was observed and in all cases, the accumulated firebrands were easily able to produce an ignition event (SI) in the wood samples. For the experiments with the full scale structure (see Fig. 6), an even greater number of firebrands were observed to accumulate, as compared to the lower profile obstacles used in these experiments. A series of photographs were also taken by increasing the exposure time on the camera to visualize the firebrand flow process over the obstacles in a very unique manner. These images are shown in Fig. 13.

4. Discussion

4.1. Ability of mesh to resist firebrand penetration into structures

Similar to prior BRI/NIST experiments that used a gable vent fitted with a mesh (6.0, 3.0, and 1.5 mm) [18], firebrands were not quenched by the presence of the mesh and would continue to burn until they were able to fit through the mesh opening. In the present work, the same behavior was observed for the smaller mesh sizes used (16×16, 1.35 mm and 20×20, 1.04 mm). The reduced scale experiments also showed the same behavior, namely firebrands were not quenched by the presence of the mesh but would continue to burn until sufficient mass loss allowed the firebrands to penetrate the mesh.

It was possible to determine the penetration ratio, for a given time interval, using the following:

$$\frac{\sum_{t=0}^{\Delta t} FB_l}{\sum_{t=0}^{\Delta t} FB_a} \times 100 \quad (1)$$

where FB_l and FB_a are the number of firebrands leaving from the mesh and the number of firebrands arriving at the mesh for a given time interval, Δt, respectively. Fig. 14 displays the penetration ratio of each mesh calculated for the duration between 110 and 115 s, when the maximum firebrand penetration was likely to occur. As shown in the figure, the firebrand penetration for the 4×4 mesh was much higher, at a given time, than for all other mesh sizes considered. As the mesh size was reduced to 10×10 (2.0 mm), the penetration ratio decreased significantly. It is interesting to note that a transition point for the ignition tests was also observed for the 10×10 (2.0 mm) mesh; a transition from SI to FI was never observed as the mesh size was reduced below 10×10 (2.0 mm).

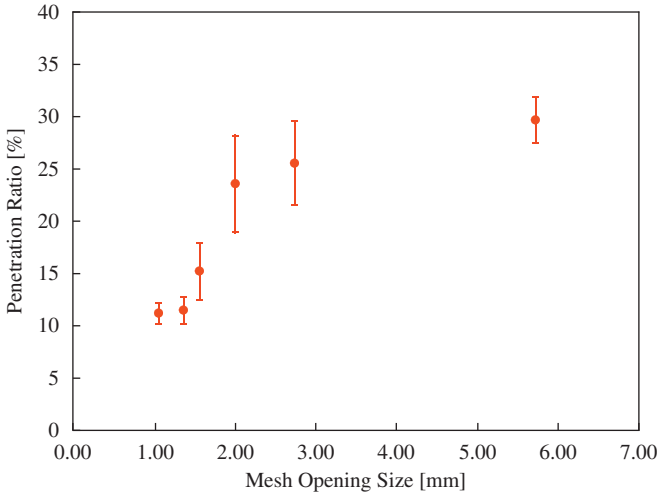

Fig. 14. Firebrand penetration ratio as a function of mesh opening size. The penetration ratio was determined based on average of three experiments at each mesh size.

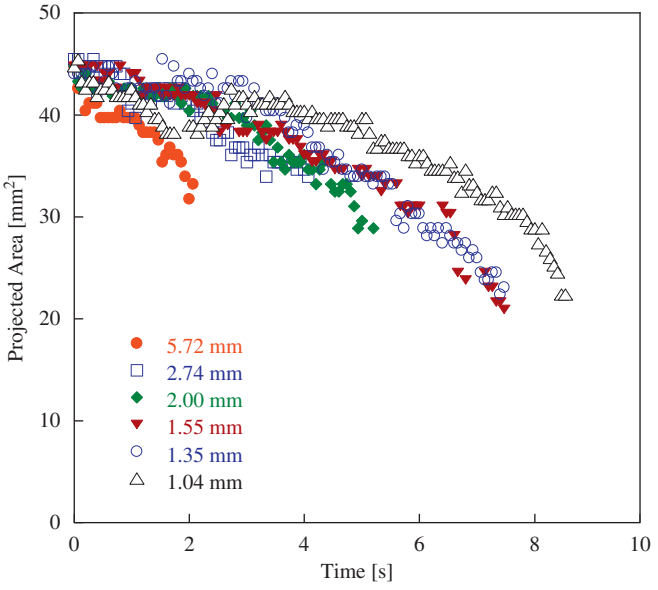

Fig. 15. Measured retention time of firebrands on a given mesh as a function of mesh size.

Another important parameter, in addition to the penetration ratio, was the retention time of firebrands as a function of mesh size. The retention time was defined as the time required for a firebrand, after arrival on a given mesh, to burn down in order to be able to pass through a given mesh opening. Fig. 15 displays these results. To determine this, the area of certain firebrands (selected randomly) was determined as a function of time for each mesh size. As can be seen from the figure, the retention time of firebrands was clearly a function of mesh size and increased as the mesh size was reduced. Therefore, as the mesh size was reduced, the penetration ratio was observed to decrease and the retention time was observed to increase.

In real WUI fires and urban fires, firebrand attack has been observed for several hours and with winds in excess of 20 m/s [27]. Therefore, the firebrand exposure conditions in these experiments are not a worst case scenario and the results presented are not conservative. Even under such liberal exposure conditions in the present experiments (four minutes), ignition was observed behind the 20×20 (1.04 mm) mesh for the fine fuels used. While mesh size reduction did mitigate ignition of bare wood crevices, the presence of fine fuels would be expected in attic spaces. When crevices were filled with fine fuels, ignitions were observed down to 14×14 (1.55 mm) mesh size, even under the conditions of these experiments.

Due to design of the FRWTF, it was not possible to test using wind speeds higher than 10 m/s. It was also not possible to increase the duration the firebrand attack using the present version of the Firebrand Generator. In real fires, the duration of firebrand attack would most likely be longer than the one simulated presently and increase the potential for a greater number of firebrands to penetrate a given mesh size. Thus, in a real fire, it is plausible that a greater number of firebrands would penetrate the mesh (due to increased firebrand attack duration and higher wind speed) and land inside structures as compared to the present experiments, providing favorable conditions for ignition. Therefore, the use of mesh to mitigate ignition is not effective and firebrand resistant vent technologies are needed. The reduced scale Dragon's LAIR facility has demonstrated that it may be used to assess the performance of such technologies to a wind driven firebrand attack.

4.2. Danger of firebrand accumulation in front of structures

Clearly, mesh was not effective in preventing firebrand penetration into building vents. Yet, the accumulation of firebrands observed using the obstacles as well as the full structure, have demonstrated that this scenario may in fact be just as dangerous to potentially ignite structures in WUI fires. These experiments demonstrate that if ignitable materials are located in front of structures, it is very easy for firebrands to accumulate and ignite materials. The subsequent ignition of materials in front of structures may in fact produce additional firebrands that would lead to even more ignitions near structures. A wide variety of ignitable materials may be found around or near structures (e.g. decks, grass, and vegetation). This paper has demonstrated the dangers of not only building vents fitted with mesh but also the ability of firebrand showers to accumulate in front of structures and easily ignite materials.

5. Summary

The BRI/NIST full scale and NIST reduced scale experiments found that firebrands were not quenched by the presence of the mesh and would continue to burn until they were able to fit through the mesh opening, even down to 1.04 mm opening. The experiments demonstrate that mesh was not effective in reducing ignition for the fine fuels tested and firebrand resistant vent technologies are needed. The results of the experiments conducted by NIST demonstrate that the reduced scale Dragon's LAIR facility was able to reproduce the results obtained from the full scale experiments conducted at BRI. These results were expected since the following parameters of Dragon's LAIR facility were specifically tailored to be similar to the full scale experiments: size and mass of firebrands generated/arriving on the mesh, mesh size, and effective area, velocity behind each mesh size used, as well as the same ignitable materials (all oven dried).

While the Dragon's LAIR facility was used to investigate firebrand penetration through building vents in this study, it is not limited to vents and may be used to expose building materials to a wind driven firebrand attack. Additional experimentation underway with the NIST Dragon's LAIR includes varying the velocity of the ignitable materials to determine ignition regime maps and developing numerical simulations of the observed ignition behavior using the NIST Wildland–Urban Interface (WUI) Fire Dynamics Simulator [28].

It is important to point out An ASTM task group on vents, organized within Subcommittee E05.14.06, External Fire Exposures, has also developed a reduced scale test method (not presently a standard) aimed at evaluating the ability of vents to resist firebrand intrusion into attic and crawl space areas. In this test method, firebrands are produced by igniting wood pieces and the firebrands are subsequently deposited on top of the vent installed in the test chamber. The vent is placed horizontally in the apparatus and air is pulled through the vent using a fan placed downstream. The mechanism of firebrands residing on top of vents and being pulled down onto vents is not representative of the actual situation. Firebrands are actually blown onto the vents themselves.

Therefore, a comparison testing protocol was undertaken, with the formal support [29] of the ASTM E05.14.06 task group, between the method developed by ASTM to the full scale experiments using the NIST Firebrand Generator at BRI's FRWTF as these full scale tests developed by BRI/NIST attempt to simulate a wind driven firebrand attack that is seen in actual WUI fires. This comparison testing protocol was undertaken to determine if the reduced scale method (ASTM) was able to capture the salient physics of firebrand penetration through building vents observed using the full scale test method. The results of comparison testing protocol are beyond the scope of this paper and the subject of a future publication.

A series of full scale experiments were also conducted to visualize the flow of firebrands around obstacles placed downstream of the NIST Dragon. Firebrands were observed to accumulate in front of these obstacles at a stagnation plane, as was observed when the structure was used, due to flow recirculation. These experiments demonstrate that if ignitable materials are located in front of structures, it is very easy for firebrands to accumulate and ignite materials. The subsequent ignition of such materials may in fact produce additional firebrands that would lead to even more ignitions near structures. The accumulation of firebrands in front of structures presents a severe threat to ignitable materials placed near structures in WUI fires.

Acknowledgments

Mr. Yu Yamamoto of the Tokyo Fire Department (Guest Researcher at BRI) and Dr. Ichiro Hagiwara of BRI are acknowledged for their support of these experiments during SLM's stay in Japan. The Dragon's LAIR experiments were conducted in the NIST Large Fire Laboratory (LFL). The assistance of the LFL staff is appreciated (Dr. Matthew F. Bundy—supervisor; Mr. Laurean DeLauter and Mr. Anthony Chakalis—Engineering Technicians).

Mr. Marco G. Fernandez, Engineering Technician (EL) constructed the support system for the Dragon's LAIR facility and carefully prepared materials needed for testing; his excellent assistance is appreciated. SLM acknowledges funding from the Science & Technology Directorate of the U.S. Department of Homeland Security.

References

[1] 2007 Annual Report of the Insurance Commissioner, California Department of Insurance (〈http://www.insurance.ca.gov〉).
[2] J.W. Mitchell, O. Patashnik, Firebrand protection as the key design element for structural survival during catastrophic wildfire fires, in: Proceedings of the 10th International Conference on Fire and Materials Conference, San Francisco, CA, 2007.
[3] A. Maranghides, W.E. Mell, A Case Study of a Community Affected by the Witch and Guejito Fires, NIST TN 1635 April 2009.
[4] F. Albini, Transport of firebrands by line thermals, Combustion Science and Technology 32 (1983) 277–288.
[5] A. Muraszew, J.F. Fedele, Statistical Model for Spot Fire Spread, The Aerospace Corporation Report No. ATR-77758801, Los Angeles, CA, 1976.
[6] C.S. Tarifa, P.P. del Notario, F.G. Moreno, On the flight paths and lifetimes of burning particles of wood, Proceedings of the Combustion Institute 10 (1965) 1021–1037.
[7] C.S. Tarifa, P.P. del Notario, F.G. Moreno, Transport and Combustion of Fire Brands Instituto Nacional de Tecnica Aerospacial Esteban Terradas, Final Report of Grants FG-SP 114 and FG-SP-146, vol 2, Madrid, Spain, 1967.
[8] S.D. Tse, A.C. Fernandez-Pello, On the flight paths of metal particles and embers generated by power lines in high winds and their potential to initiate wildfires, Fire Safety Journal 30 (1998) 333–356.
[9] J.P. Woycheese, Brand Lofting and Propagation for Large-Scale Fires, Ph.D. Thesis, University of California, Berkeley, 2000.
[10] J.P. Woycheese, Wooden disk combustion for spot fire spread, in: S. Grayson (Ed.), Ninth Fire Science and Engineering Conference Proceedings (INTERFLAM) Interscience Communications, London, 2001, pp. 101–112.
[11] I.K. Knight, The design and construction of a vertical wind tunnel for the study of untethered firebrands in flight, Fire Technology 37 (2001) 87–100.
[12] R. Anthenien, S.D. Tse, A.C. Fernandez-Pello, On the trajectories of embers initially elevated or lofted by small scale ground fire plumes in high winds, Fire Safety Journal 41 (2006) 349–363.
[13] K. Himoto, T. Tanaka, Transport of disk shaped firebrands in a turbulent boundary layer, Fire Safety Science 8 (2005) 433–444.
[14] N. Sardoy, J.L. Consalvi, A. Kaiss, B. Porterie, A.C. Fernandez-Pello, Modeling transport and combustion of firebrands from burning trees, Combustion and Flame 150 (2007) 151–169.
[15] N. Sardoy, J.L. Consalvi, A. Kaiss, A.C. Fernandez-Pello, B. Porterie, Numerical study of ground-level distribution of firebrands generated by line-fires, Combustion and Flame 154 (2008) 478–488.
[16] S. Kortas, P. Mindykowski, J.L. Consalvi, H. Mhiri, B. Porterie, Experimental validation of a numerical model for the transport of firebrands, Fire Safety Journal 44 (2009) 1095–1102.
[17] H. Wang, Analysis on downwind distribution of firebrands sourced from a wildland fire, Fire Technology Special Issue: Wildland Fires in Fire Safety Engineering 47 (2011) 321–340.
[18] S.L. Manzello, J.R. Shields, J.C. Yang, Y. Hayashi, D. Nii, On the use of a firebrand generator to investigate the ignition of structures in WUI Fires, in: Proceedings of the 11th International Conference on Fire Science and Engineering (INTERLFAM), Interscience Communications, London, 2007, pp. 861–872.
[19] S.L. Manzello, J.R. Shields, Y. Hayashi, D. Nii, Investigating the vulnerabilities of structures to ignition from a firebrand attack, in: B. Karlsson (Ed.), Fire Safety Science—Proceedings of the Ninth International Symposium, vol. 9, IAFSS, 2008, pp. 143–154.
[20] S.L. Manzello, Y. Hayashi, Y. Yoneki, Y. Yamamoto, Quantifying the vulnerabilities of ceramic tile roofing assemblies to ignition during a firebrand attack, Fire Safety Journal 45 (2010) 35–43.
[21] S.L. Manzello, S.H. Park, J.R. Shields, Y. Hayashi, S. Suzuki, Comparison Testing Protocol for Firebrand Penetration through Building Vents: Summary of BRI/NIST Full Scale and NIST Reduced Scale Results, NIST, TN 1659, January 2010.
[22] S.L. Manzello, S.H. Park, J.R. Shields, S. Suzuki, Y. Hayashi, Quantifying wind driven firebrand penetration into building vents using full scale and reduced scale experimental methods, in: Proceedings of the 12th International Conference on Fire Science and Engineering (INTERLFAM), Interscience Communications, London, 2010, pp. 1189–1200.
[23] S.L. Manzello, J.R. Shields, T.G. Cleary, A. Maranghides, W.E. Mell, J.C. Yang, Y. Hayashi, D. Nii, T. Kurita, On the development and characterization of a firebrand generator, Fire Safety Journal 43 (2008) 258–268.
[24] K. McGrattan, R. McDermott, S. Hostikka, J. Floyd, Fire Dynamics Simulator (Version 5) User's Guide', NIST Special Publication 1019-6, (April 2010).
[25] S.L. Manzello, A. Maranghides, W.E. Mell, Firebrand generation from burning vegetation, International Journal of Wildland Fire 16 (2007) 458–462.
[26] S.L. Manzello, A. Maranghides, J.R. Shields, W.E. Mell, Y. Hayashi, D. Nii, Mass and size distribution of firebrands generated from burning Korean pine (*Pinus koraiensis*) trees, Fire and Materials Journal 33 (2009) 21–31.
[27] J.W. Mitchell, Power lines and catastrophic wildland fire in Southern California, in: Proceedings of the 11th International Conference on Fire and Materials, San Francisco, CA, 2009, pp. 225–238.
[28] W.E. Mell, A. Maranghides, R. McDermott, S.L. Manzello, Numerical simulation a experiments of burning douglas-fir trees, Combustion and Flame 145 (2009) 2023–2041.
[29] Official minutes ASTM E05.14 external fire exposure, June 17, 2009 (〈http://www.astm.org〉).